A Quantum Chemical Study of Intramolecular Charge Transfer in a Closely-Spaced, Donor−Acceptor Molecule

Ata Amini and Anthony Harriman*

Department of Chemistry, Molecular Photonics Laboratory, Bedson Building, University of Newcastle, Newcastle upon Tyne, NE1 7RU, United Kingdom

Received: October 9, 2003; In Final Form: November 30, 2003

This investigation explores the use of contemporary quantum chemistry to mimic the light-induced, intramolecular charge-transfer processes that occur in 2-methyl-2,3-dihydrobenz[d,e]isoquinoline (DHBIQ) in polar solvents. Thus, the computed excited-state manifold, comprising two locally excited π,π^* singlets, a locally excited π,π^* triplet, and a charge-transfer (CT) state, is in excellent agreement with the experimental findings. It is shown that, whereas the energies of the various locally excited states are insensitive to molecular geometry and environment, the energy of the CT state depends markedly on structure and solvent polarity. The most favorable charge-transfer interactions occur within a distorted geometry that is midway between the axial and equatorial conformers identified for the ground state. The calculated nuclear and solvent reorganization energies are in good agreement with prior experimental work. Molecular dynamics simulations were employed to estimate the change in Gibbs free energy accompanying charge transfer and this latter value, used in conjunction with the reorganization energy, allows reproduction of the experimental activation energy. Finally, the electronic coupling matrix element for charge transfer was computed by identifying the intersection point for potential energy surfaces associated with the CT state and the lowest-energy π,π^* excited singlet state. The derived value ($T_{DA} = 206$ cm^{-1}) is close to the experimental result ($T_{DA} = 140$ cm^{-1}) obtained by application of classical Marcus theory. Overall, it is concluded that quantum chemical methods allow meaningful calculation of the parameters controlling the rate of charge transfer in this system.

Introduction

Marcus theory describes electron transfer between donor and acceptor species.[1] It is most readily applicable to cases of intramolecular electron transfer occurring within geometrically constrained molecules dissolved in a polar solvent. Under such conditions, electron transfer is accompanied by modest structural changes in both solute and surrounding solvent, especially for those cases where the reactants are neutral. These structural changes can be conveniently represented by separate nuclear and solvent reorganization energies and, when combined with the thermodynamic driving force for the electron-transfer process, provide the activation energy for the overall reaction.[2] Innumerable experimental studies have addressed various issues relating to Marcus theory and, in particular, have determined how the rate of electron transfer depends on thermodynamic parameters[3] and solvent dynamics.[4] Parallel to this experimental work, many research groups have started to conduct quantum chemical studies aimed at evaluating some of the parameters that control the rate of electron transfer in proteins,[5] polar solvents,[6] and solid matrices.[7] An especially challenging area for quantum chemistry concerns understanding the so-called "twisted" intramolecular charge-transfer (TICT) state[8] where the electron-transfer step is accompanied by a change in molecular geometry.[9] Such systems often comprise two subunits that alternate between strongly coupled planar and weakly coupled orthogonal orientations under illumination. The most interesting feature of these TICT states concerns the minimum overlap behavior of the orthogonal structures. When the molecular geometry is constrained, it is not possible for the TICT state to attain the fully orthogonal structure but there still remains the tendency to minimize orbital overlap. Despite being studied for about four decades, the TICT process is still quite poorly understood.[10]

In particular, density functional theory with single configuration interaction[11] has been applied to TICT states and the self-consistent reaction field model[12] has been used in semiempirical methods to compute properties of the various excited states involved in such systems.[13] Other studies have examined TICT formation using CNDO/S-CI,[14] CS-INDO,[15] PPP,[16] and ab initio methods.[17] There is also a growing interest in the application of molecular dynamics and quantum dynamics simulations to electron-transfer processes.[18] These latter approaches permit calculation of adiabatic potential energy surfaces and vertical energy gaps that, in turn, can be used to derive thermodynamic properties.[19] Solvation dynamics can also be studied by non-equilibrium MD simulations.[20] In most cases, the computational studies provide support for TICT formation but do not discriminate between finer details of the charge-transfer mechanism.[21]

Some time ago, we described TICT formation in a geometrically constrained, donor−acceptor molecule, 2-methyl-1,3-dihydrobenz[d,e]isoquinoline (DHBIQ), and reported a full kinetic analysis for this system.[22] Thus, UV illumination results in formation of a locally excited π,π^* singlet state that fluoresces strongly in nonpolar solvents. Rapid intramolecular charge transfer occurs in polar solvents, leading to formation of a radical ion pair that survives for a few nanoseconds before undergoing charge recombination to produce a mixture of ground state and

* To whom correspondence should be addressed. E-mail: anthony.harriman@ncl.ac.uk.

10.1021/jp037039l CCC: $27.50
Published on Web 01/27/2004

locally excited π,π^* triplet state. It was postulated that charge transfer is accompanied by modest structural modification around the donor N atom but this point was not confirmed by experiment. We now return to this system and show that modern quantum chemical approaches can give a meaningful representation of the structural changes associated with charge transfer. Such methods also permit facile calculation of the overall reorganization energy[23] and the Gibbs free-enegy change[24] accompanying charge transfer. When combined with time-resolved laser spectroscopic studies,[22,25,26] the computational work provides deep insight into the electron-transfer mechanism. Indeed, it appears that both quantum mechanical and molecular dynamics methods give reasonable estimates for the reorganization energy while the latter method can be used also to estimate the overall change in Gibbs free energy.

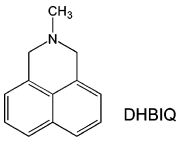

DHBIQ

Methods

Structures for DHBIQ in different electronic states were calculated by the PM3-CI method,[27] with 12 electrons and 12 molecular orbitals lying within the active space, using Quantum Cache version 4.4.[28] Preliminary calculations showed that increasing the number of molecular orbitals in the active space had no real effect on the accuracy of the results. Output from the PM3-CI calculations was imported into Gaussian 98[29] to allow ab initio HF/3-21 g* and MP2/3-21G* calculation[30] of the nuclear reorganization energy of DHBIQ and of the individual components. Solvent reorganization energies were computed by the finite difference Poisson−Boltzmann (FDPB)[31] method using the Mulliken partial charges taken from the PM3-CI calculations and using INSIGHT-II.[32] Water was treated as a continuum solvent. Total reorganization energies and changes in Gibbs free energy ($\Delta G°$) were calculated by molecular dynamics simulation of the hydrated system using CHARMM.[33] The required input files and all visualization procedures used with CHARMM were made with INSIGHT-II. Calculation of the electronic coupling matrix element was carried out by placing a single water molecule at a distance d from the plane of the molecule and computing energies of the first excited singlet state (S_1) and of the charge-transfer (CT) state using the PM3-CI method. The distance was changed systematically until reaching the intersection point for the relevant potential energy surfaces, where the coupling element is numerically equal to half the minimum energy gap.

Results and Discussion

Electronic and Geometric Structures. The experimental studies[22] devoted to exploring the photophysical properties of DHBIQ in a range of solvents of differing polarity identified two π,π^* excited singlet states localized on the naphthalene ring and situated at comparable energies. In polar solvents, electron transfer occurs from the N atom of the amino donor to the lowest-energy π,π^* excited singlet state to form a relatively long-lived, charge-transfer (CT) state. This latter species decays by way of charge recombination to form a mixture comprising the π,π^* excited triplet state and the ground state. As such, the CT state must be situated at an energy intermediate between those of the locally excited singlet and triplet states. Furthermore, the CT state cannot be detected in nonpolar solvents so that, under such conditions, it must lie at an energy above that of the locally excited singlet state.[22] Before attempting to calculate the thermodynamic parameters pertinent to intramolecular charge transfer in DHBIQ, it is necessary to reproduce the above features and to compute reasonable structures for the relevant electronic states.

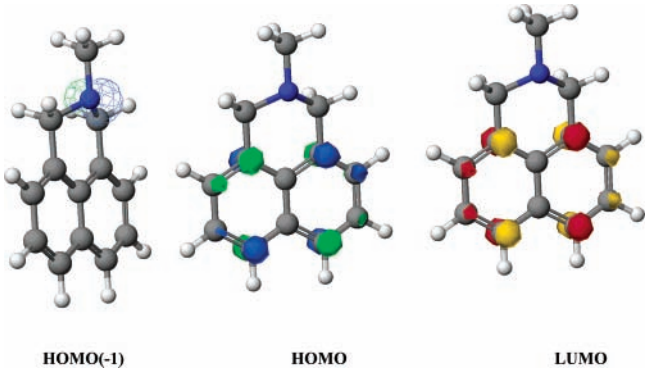

Figure 1. Molecular orbitals involved in the various n,π^* and π,π^* transitions computed for DHBIQ. Both HOMO and LUMO are localized on the naphthalene ring but HOMO(−1) is centered on the N atom.

It is recognized that DHBIQ undergoes fast N inversion so that the ground state exists as a mixture of axial and equatorial conformers. Calculations showed that the barrier to N inversion is only 1.93 kcal mol^{-1} and that, because of stereochemical factors,[34] the equatorial conformer is slightly favored over the axial conformer. The structure of the equatorial conformer in water and in vacuo was established by computation at the PM3-CISD level to identify the appropriate electronic transitions. Thus, systematic searching through the computed molecular orbitals indicated that the highest occupied molecular orbital (HOMO) was of π-character and was localized on the naphthalene ring (Figure 1). The corresponding lowest unoccupied molecular orbital (LUMO) was of π^*-character and again was localized on the aromatic nucleus. Consequently, transitions between the HOMO and LUMO can be designated as primarily π,π^* in nature. Whereas LUMO(1) remains of π^*-character, HOMO(−1) corresponds to the lone-pair localized on the N-atom of the amino group (Figure 1). Transitions from this latter MO to the virtual π^* orbitals localized on the naphthalene ring are formally of n,π^* character but correspond to formation of the CT state. In subsequent MO calculations, we considered a total of 12 MOs and 12 electrons, taking into account both single and double excitations. It appears that configurations 5−10 involve transitions from HOMO(−1) to the virtual π^* orbitals localized on naphthalene. As such, states with significant contributions from these configurations should be of n,π^* character.

Using the PM3-CISD calculated equatorial geometry for the DHBIQ ground state and the optimized structure for each excited state, calculations were made to compute the energies of the first nine excited states (Table 1) in both water and in vacuo. The ground-state structure is insensitive to the polarity of the surrounding medium and, as a consequence, most of the computed excitation energies remain closely comparable in water and in vacuo. This is in accord with the experimental studies,[22] which found that the absorption spectrum was hardly affected by changes in solvent polarity. These studies also found a small Stokes' shift for the locally excited singlet state, indicating similar geometries for ground and first-excited singlet states.[35] Indeed, the calculated structures for the first-excited singlet and triplet states remain very similar to that of the ground state and

TABLE 1: Vertical Excitation Energies from PM3-CISD Calculations Carried Out on the Optimized (Equatorial) Ground-State and Excited-State Structures of DHBIQ in Vacuo and in Water

state number	multiplicity	energy (cm^{-1}) in vacuo	contribution of the configurations in vacuo	energy (cm^{-1}) in water	contribution of the configurations in water
1	singlet	0	0.98 of 1	0	0.98 of 1
2	triplet	20 480	0.67 of 2	20 400	0.69 of 2
3	triplet	26 450	0.56 of 3 and 0.43 of 11	25 460	0.62 of 3 and 0.31 of 11
4	singlet	31 800	0.5 of 3 and 0.49 of 11	31 710	0.52 of 3 and 0.46 of 11
5	triplet	32 100	0.43 of 3 and 0.54 of 11	32 060	0.67 of 12
6	triplet	32 260	0.7 of 12	32 190	0.33 of 3 and 0.56 of 11
7	singlet	32 520	0.62 of 2 and 0.32 of 12	32 500	0.62 of 2 and 0.31 of 12
8	triplet	34 895	0.64 of 4 and 0.25 of 5	34 290	0.63 of 4 and 0.19 of 5
9	singlet	39 310	0.67 of 5	29 030	0.58 of 5

are little affected by changes in solvent polarity. Repeating the calculations for the axial conformer gave essentially the same excitation energies for the first two singlet excited states and for the two lowest-energy triplet states.

The accuracy of these calculations can be assessed by comparing the computed energies with those available from absorption and emission spectroscopy.[22] Thus, the absorption spectrum has been analyzed to show 0,0 transitions for the ^1L_b and ^1L_a singlet states at 322 and 310 nm, respectively, and a strongly allowed transition to the ^1B_b state centered at 222 nm. These values can be compared with the theoretical estimates of 315 (^1L_b), 308 (^1L_a), and 240 (^1B_b) nm. Weak phosphorescence was detected in a frozen glass at 77 K, with the 0,0 band being located at 485 nm. In contrast, calculations place the spin-forbidden S_0-T_1 transition at 488 nm. On this basis, it appears that the MO calculations correctly identify and locate the first two locally excited singlet states and the first triplet state. It should be stressed that these computed excitation energies are the same for the ground-state equatorial and axial conformers.

The third singlet excited state arises primarily because of a transition from HOMO(−1) to LUMO and, as such, corresponds most closely to excitation to the CT state (Figure 1). The computed structure of this CT state in vacuo remains similar to those of the various π,π^* excited states but, in marked contrast to the other species, there is a significant change in optimized geometry when the CT state is studied in water. The structural differences for the CT state in vacuo and in water are shown in Figure 2 and are compared with the computed structures for

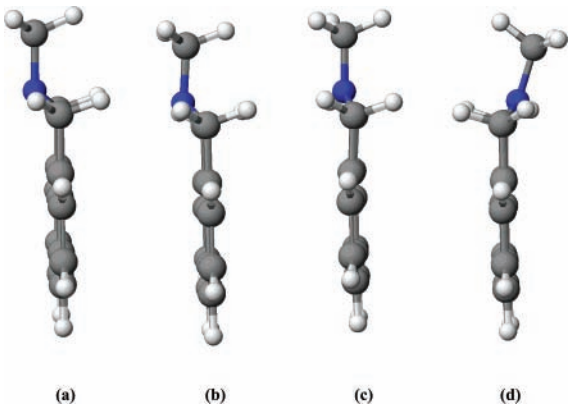

Figure 2. Computed PM3-CISD structures of (a) the ground state, (b) first-excited singlet state, and (c) the charge-transfer state in vacuo. Panel (d) shows the computed structure for the CT state in water.

the equatorial conformers of the ground state and lowest-energy excited singlet state. In water, the CT state adopts a structure that is essentially midway between axial and equatorial geometries. This distorted form is the most stable geometry for the CT state in a polar solvent and is reached regardless of starting geometry. The importance of a polar solvent to stabilize the CT state is illustrated in Figure 3, which shows the effect of

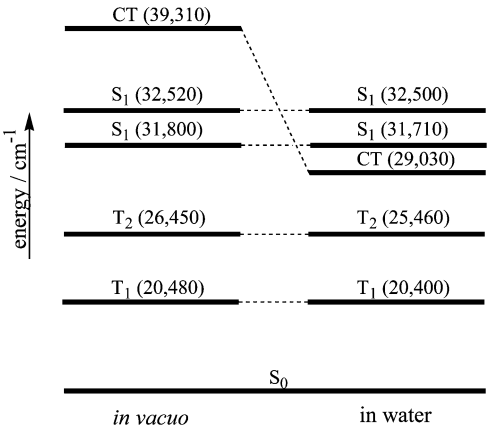

Figure 3. Effect of water on the energies of the first-excited singlet and triplet states and of the CT state. Energies are given in units of cm^{-1}.

water on the energies of the various excited states as computed by single-point calculation for the optimized structures. Whereas the energies of both S_1 and T_1 remain almost unaffected by the nature of the surrounding solvent, as expected for naphthalene-like π,π^* excited states,[36] the energy of the CT state falls markedly in water with respect to vacuum. In water, the energy of the CT state lies between those of S_1 and T_1, in exact accordance with the experimental results. The calculations also imply that the solvent-stabilized CT state evolves from the Franck−Condon state reached by vertical excitation.

Nuclear Reorganization Energy. It is generally accepted that the total reorganization energy (λ_T) accompanying a charge-transfer process comprises terms related to nuclear (λ_N) and solvent (λ_S) rearrangements.[1,2] For DHBIQ in acetonitrile at room temperature, λ_T was estimated to be ca. 0.9 eV by analysis of the emission spectrum attributed to the CT state.[22] This particular reorganization energy refers to relaxation of the solvent-stabilized CT state to the ground state. By using a simple dielectric continuum model, and assuming spherical reactants, λ_S was estimated to be ca. 0.6 eV so that, by difference, λ_N must be ca. 0.3 eV.[22] These derived values are necessarily crude and attempts were made to compute both λ_N and λ_S to refine our understanding of the charge-transfer mechanism and to compare experimental and theoretical values.

Two different methods were used to calculate the nuclear reorganization energy. First, to calculate λ_N for conversion of S_1 into the stabilized CT state, the geometry was optimized for the first-excited singlet state and the energy of this species (E_{R1}) was computed. The energy of the CT state (E_{P1}) was subsequently calculated for the same geometry. Next, the structure of the CT state was optimized and the energy at the optimized

TABLE 2: Nuclear Reorganization Energies Calculated for the Isolated Donor and Acceptor Subunits

method	donor/eV	acceptor/eV	total/eV
HF/3-21G*	0.377	0.131	0.508
PM3	0.380	0.133	0.513
MP2/3-21G*	0.377	0.120	0.497

geometry (E_{P2}) was calculated. Finally, the energy of the locally excited singlet state (E_{R2}) was calculated for the geometry optimized for the CT state. All calculations were made for the solute in a bath of water molecules. The nuclear reorganization energy is given simply as the average difference between the relevant pairs of energies: $E_{R2} - E_{R1}$ or $E_{P2} - E_{P1}$ or an average of these two values. Using the above-mentioned PM3-CISD calculations to set the optimized structures, we find $\lambda_{N1} = E_{R2} - E_{R1} = 0.34$ eV and $\lambda_{N2} = E_{P2} - E_{P1} = 0.58$ eV. The average value, calculated by this method, becomes $\lambda_N = 0.46 \pm 0.12$ eV.

In the second method, λ_N for relaxation of the CT state to the ground state was calculated by considering geometry changes that accompany oxidation or reduction of the isolated donor (e.g., trimethylamine) and acceptor (e.g., 1,8-dimethylnaphthalene) subunits. During charge transfer, the donor becomes oxidized and the acceptor becomes reduced such that λ_N can be considered as the sum of the two individual energy terms. These individual energies were computed by both semiempirical PM3[37] methods and by ab initio HF/3-21 g* and MP2/3-21 g* calculations[38] (with the optimized geometries coming from CIS/3-21 g* calculations). The results are collected in Table 2, where it is seen that structural distortion within the donor unit makes the major contribution to the overall λ_N. Closely comparable reorganization energies are found by the different computational methods. The average value ($\lambda_N = 0.5$ eV) is similar to that found for formation of the CT state from S_1 and is in fair agreement with the experimental estimate ($\lambda_N = 0.3$ eV).

Solvent Reorganization Energy. The finite difference Poisson−Boltzmann (FDPB) method[31] allows calculation of changes in the electrostatic solvation free energies (ΔG_{ele}) according to the following equation:

$$\Delta G_{ele} = \frac{1}{2}\sum_i q_i[\varphi_i(\epsilon_s - \epsilon_v)] \quad (1)$$

Here q_i is the charge resident on atom i, ϵ_s and ϵ_v are the dielectric constants in the presence of a continuum solvent and in vacuo, respectively, while φ_i is the electrostatic free energy of atom i. The solvent reorganization energy (λ_S) is the difference in solvation free energy between the ground state and the CT state.[1] This term, which is expected to depend on the polarity of the surrounding solvent, can be calculated by the FDPB method using the following expression:

$$\lambda_o = \frac{1}{2}\sum_i \Delta q_i[\varphi_i(\epsilon_s - \epsilon_\nu)] \quad (2)$$

The electrostatic potential can be calculated from the Poisson−Boltzmann equation:

$$\nabla\cdot[\epsilon(r)\cdot\nabla\cdot\varphi(r)] + 4\pi\rho_{tot}(r) = 0 \quad (3)$$

Here, ρ_{tot} is the distance-dependent charge density and the first term shows the change of the electric displacement that is relevant to the dielectric constant and change of electrostatic potential. The former term contains contributions from interactions between atoms in the molecular backbone and from the distribution of dipoles in solution, which can be found by the Boltzmann distribution model. This model leads to the linear form of the Poisson−Boltzmann equation:

$$\nabla\cdot[\epsilon(r)\cdot\nabla\cdot\varphi(r)] - \bar{\kappa}^2(r)\varphi(r) = -4\pi\rho(r) \quad (4)$$

where κ is the modified Debye−Hückel screening factor and ρ is the charge density of the solute. Further details of this method can be found elsewhere.[39]

TABLE 3: Solvent Reorganization Energies Calculated by the FDPB Method and Essential Input Data for Solvents of Differing Polarity

solvent	ϵ_S[a]	Onsager radius/Å	$E_{CT\ STATE}$[b]/ kcal mol^{-1}	E_{S0}[c]/ cal mol^{-1}	λ_S[d]/eV
water	80	1.4	−21.48	−9.29	0.53
acetonitrile	37	2.5	−20.05	−8.58	0.50
cyclohexane	2	2.78	−6.11	−2.01	0.18

[a] Static dielectric constant. [b] Solvation energy for the CT state. [c] Solvation energy for the ground state. [d] The derived λ_S values refer to relaxation of the CT state to the ground state, S_0.

The main results, together with essential input data, are collected in Table 3. This particular calculation refers to relaxation of the stabilized CT state to the ground state and, as expected, λ_S increases with increasing solvent polarity, being rather small in cyclohexane. The value found in acetonitrile ($\lambda_S = 0.50$ eV) indicates that the solvent and nuclear components make essentially equal contributions to the total reorganization energy in polar solvents. The overall value ($\lambda_T = 1.0$ eV) is in fair agreement with the experimental estimate[22] of $\lambda_T = 0.9$ eV made on the basis of the emission maximum. This latter value is necessarily crude and should not be taken as an indication of a serious mismatch with the calculated value. Even so, the reliability of the computed value is set by the quality of the Mulliken partial charges used for the calculation. The same calculation made for evolution of the CT state from S_1 gives $\lambda_S = 0.48$ eV in acetonitrile solution. The similarity between these two λ_S values might be expected on the basis of comparable geometries and partial charges for S_1 and the ground state.

Change in Gibbs Free Energy. Molecular dynamics and quantum dynamics simulations, which have little restriction on the number of atoms under consideration, have been used to calculate thermodynamic driving forces for electron-transfer processes occurring in various organic, inorganic, and biological systems.[40] Here, we have used the MD technique to calculate the change in Gibbs free energy ($\Delta G°$) accompanying transformation of S_1 into the CT state and also to provide a further estimate of the total reorganization energy (λ_T) associated with this step. The approach used involves a classical dynamics simulation of a solvated system with added water molecules within a box. It is necessary to first define potential energy surfaces for the initial state, assumed to be S_1, and the final state, taken to be the solvent-stabilized CT state, and to establish partial electronic charge distributions for each state. The solute molecule was placed in a cubic box of size $25 \times 25 \times 25$ Å^3 with TIP3[41] water molecules. The periodic boundary condition was applied so as to keep the solvent around the solute, and the system was minimized for 1000 steps using the adopted basis Newton−Raphson method.[42] The MD simulation was run for 50 ps at 300 K with the Langevin dynamics algorithm[45] and a time step of 1 fs to equilibrate the system before performing separate simulations for the system before and after charge transfer. The calculated trajectories on the two potential

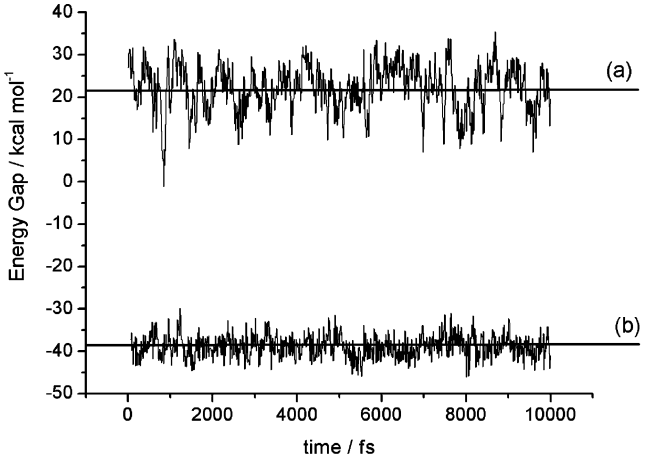

Figure 4. Time dependence of the energy gap between potential energy surfaces starting from (a) S_1 and (b) the CT state, as derived from molecular dynamics simulations carried out for both states. The averaged energy gaps are (a) 22.00 and (b) -38.85 kcal mol^{-1}, respectively, starting from S_1 and the CT state.

energy surfaces correspond to thousands of possible conformations of the system. For each conformation, calculations were made for the energy of the system before electron transfer (E_R) and after electron transfer (E_P). The resultant energy gap, $\Delta E_R = E_P - E_R$, corresponds to the energy required to transfer an electron from the reactant to the product. An identical calculation is carried out for the simulation on the second potential energy surface to compute the analogous ΔE_P for each time increment.

The calculated energy gaps for the two potential energy surfaces are shown in Figure 4 as a function of simulation time. Taking the averaged energy gaps for the initial ($\langle \Delta V \rangle_i$) and final ($\langle \Delta V \rangle_f$) states, as run over prolonged simulations, it becomes possible to estimate λ_T and $\Delta G°$ according to the following expressions:

$$\lambda_T = \frac{1}{2}(\langle \Delta V \rangle_f - \langle \Delta V \rangle_i) \tag{5}$$

$$\Delta G^o = \frac{1}{2}(\langle \Delta V \rangle_f + \langle \Delta V \rangle_i) \tag{6}$$

According to the averaged values shown in Figure 4, and making use of eqs 5 and 6, the MD simulations provide estimates for λ_T of 1.32 eV and for $\Delta G°$ of -0.37 eV. It is reassuring that these values retain appropriate signs, especially for $\Delta G°$, but the two estimates are correlated. The value obtained for the total reorganization energy is larger than that calculated earlier ($\lambda_T = 1.0$ eV) and exceeds the experimental value ($\lambda_T = 0.9$ eV) by ca. 40%. Even so, the derived λ_T is not unreasonable. Using reduction potentials measured for the isolated donor and acceptor species, $\Delta G°$ has been estimated as -0.35 eV.[22] Consequently, the calculated value ($\Delta G° = -0.37$ eV) is in very close agreement with the experimental result. This is doubtless fortuitious since the dynamics simulations clearly overestimate λ_T but it is important to note that this method provides a useful route to estimating activation energies for electron-transfer processes. Thus, using classical Marcus theory[1,2] with the results of the MD simulations, we find the change in free energy of activation ($\Delta G^{\#}$) for charge transfer within DHBIQ to be 0.17 eV, compared to the experimental value of 0.08 eV. Using $\lambda_T = 1.0$ eV, as obtained earlier, $\Delta G^{\#}$ falls to 0.10 eV and is now well within the experimental range.

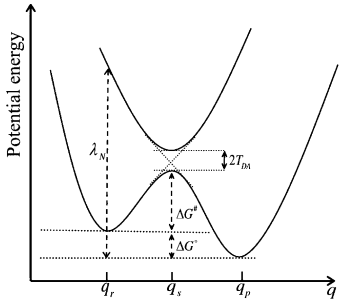

Figure 5. Schematic representation of the potential energy curves involved in light-induced charge transfer in DHBIQ along the generalized nuclear coordinate (q) in the ground state (q_R), first-excited singlet state (q_S), and the CT state (q_P). The terms indicated on the diagram refer to the nuclear reorganization energy (λ_N), the activation free-energy change ($\Delta G^{\#}$), and the change in Gibbs free energy ($\Delta G°$) accompanying charge transfer. The minimum energy gap corresponds to twice the electronic coupling matrix element (T_{DA}). The generalized coordinate refers primarily to structural changes around the amino N atom.

Electronic Coupling Matrix Element. The preceding sections allow computation of the change in free energy of activation for intramolecular charge transfer in DHBIQ and further illustrate the importance of small geometry changes accompanying electron transfer. The calculated parameters are in good agreement with those derived by experiment, especially when due consideration is given to the uncertainties associated with the experimental work. The remaining term needed to fully express the rate of intramolecular charge transfer in DHBIQ is the electronic coupling matrix element (T_{DA}). It is the calculation of T_{DA} that presents the most daunting challenge to contemporary quantum chemistry and it is also the most difficult parameter to determine by experiment. A few methods are available by which to compute T_{DA}. Thus, McConnell has developed a second-order perturbation theory to find the energy gap between the donor and the connector units and to compute the individual atomic orbital coefficients needed to calculate T_{DA}.[44] Other methods include Dyson's equation-based approach,[45] extended Hückel semiempirical methods,[46] and the application of molecular dynamics[47] to solve the Green's function.[48] Here, we use a different approach and attempt to interrogate the intersection point between potential energy surfaces for the initial state, assumed to be S_1, and the final state, taken as the CT state (Figure 5). As the energies of the two states approach each other, we encounter the avoided crossing region where the energy gap is at a minimum. The required T_{DA} is taken as half the minimum energy gap.[49]

Thus, consider a system comprising a donor with a wave function |D> and an acceptor having a wave function |A>. The total wave function for the system can be written as a linear combination of these two wave functions with coefficients c:

$$\psi = c_1|A\rangle + c_2|D\rangle \tag{7}$$

On the basis of the variational theorem,[50] the energy of this system can be found by solving the following secular equation:

$$\begin{bmatrix} H_{11} - E & H_{21} \\ H_{12} & H_{22} - E \end{bmatrix} \begin{bmatrix} c_1 \\ c_2 \end{bmatrix} = 0 \tag{8}$$

Here, H_{ij} is the electronic Hamiltonian between orbitals i and j. The solution for this secular determinant is as follows:

$$E_{\pm} = \frac{(E_D + E_A) \pm \sqrt{(E_D - E_A)^2 + 4|T_{DA}|^2}}{2} \tag{9}$$

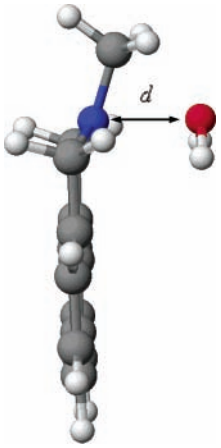

Figure 6. Pictorial representation of the method used to calculate the size of the electronic coupling matrix element. The distance (d) between the water molecule and DHBIQ was varied systematically until the potential energy curves reached the crossing point.

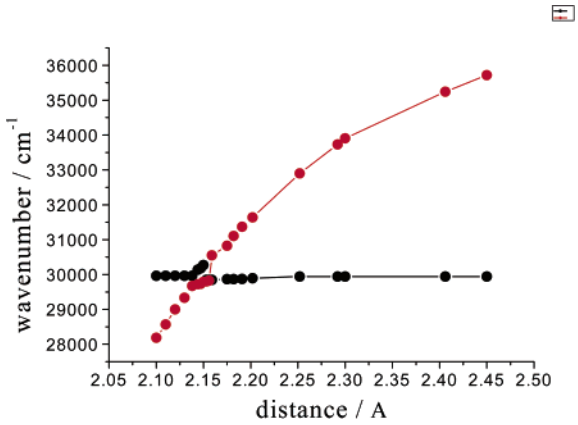

Figure 7. A plot of the excitation energy of S_1 (black circles) and the CT state (red circles), expressed in terms of wavenumber, as a function of the distance between the added water molecule and DHBIQ. The minimum energy gap is used to calculate T_{DA}. The wavenumbers are taken from PM3-CISD calculations.

where

$$E_D = H_{11} = \langle D|H|D\rangle$$

$$E_A = H_{11} = \langle A|H|A\rangle$$

$$T_{DA} = H_{12} = H_{21} = \langle D|H|A\rangle \qquad (10)$$

Suppose the system reaches the special condition whereby the initial and final states possess identical energies. Under such conditions, $E_D = E_A$ in eq 9 and we have

$$T_{DA} = \frac{1}{2}(E_+ - E_-) \qquad (11)$$

To bring the system to resonance, a single molecule of water was added to the system comprising a DHBIQ molecule held at fixed coordinates (Figure 6). The distance, d, between the two molecules was varied systematically over a relatively wide range. For each value of d, the exact energies of S_1 and the CT state were calculated at the PM3-CISD level with 24 molecular orbitals in the active space (Figure 7). As expected from earlier calculations, the presence of a water molecule has essentially no effect on the energy of S_1 but greatly perturbs the energy of the CT state. In fact, the energy of the CT state decreases smoothly as the water molecule approaches the solute. The

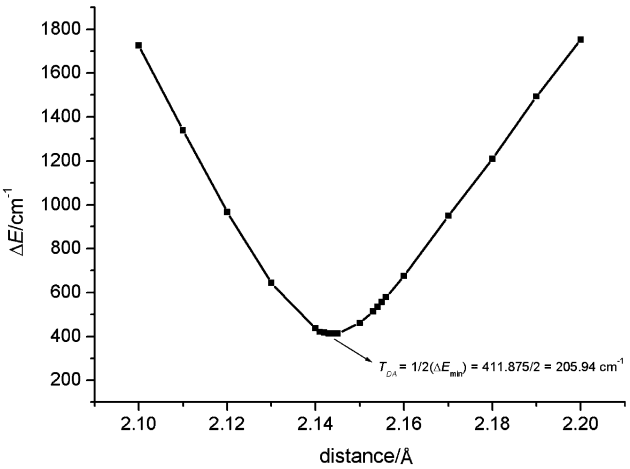

Figure 8. The effect of distance d on the energy gap between S_1 and the CT state for the results of the PM3-CISD calculations shown in Figure 7. The minimum energy gap corresponds to twice the electronic coupling matrix element.

intersection point is reached at $d = 2.143$ Å. At this distance, we would expect surface hopping to take place. Expressing the results in the form of a plot of the energy gap (ΔE) between the two states as a function of distance d (Figure 8) indicates that the minimum energy gap is 412 cm^{-1}. As such, the electronic coupling matrix element T_{DA} has an approximate value of 206 cm^{-1}. The derived value for ΔE does not depend on the initial orientation or placement of the water molecule.

The experimental study concluded[22] that T_{DA} was about 140 cm^{-1} by expressing the measured activation energy for intramolecular charge transfer in terms of classical Marcus theory.[1] As such, the calculated value is in close agreement. This similarity is rendered more surprising by the realization that the rate of charge transfer is close to the anticipated adiabatic solvent-controlled regime[51] where classical Marcus behavior might not hold.[2] The comparability between theory and experiment suggests that charge transfer in DHBIQ is covered by Marcus theory. Indeed, taking the calculated T_{DA} of 206 cm^{-1}, together with an activation energy of 0.10 eV and a total reorganization energy of 1.0 eV, the rate constant for charge transfer is calculated to be 2.2×10^{11} s^{-1}, compared to the experimental estimate of 2.5×10^{11} s^{-1}.

Conclusion

Using contemporary quantum chemical approaches, it has been possible to compute reasonable estimates for the nuclear and solvent reorganization energies, the change in Gibbs free energy, the activation energy, the electronic coupling matrix element, and the rate constant for intramolecular charge transfer in DHBIQ. Considering that charge transfer occurs at the excited state level, this is a nontrivial task and the agreement between theory and experiment is remarkably good for all the calculated parameters. In particular, the calculated rate constant is very similar to the measured value. We have also been able to reproduce the excited state manifold and correctly position the CT state with respect to the locally excited singlet and triplet states in both polar and nonpolar environments. The methods used are general and do not require extensive computation time. They should be applicable to fairly large systems.

The calculations also provide additional insight into the proposed geometry changes that accompany charge transfer in this system. The energies of S_1, S_2, and T_1, these being π,π^* excited states localized on naphthalene, are insensitive to

changes in the geometry around the amino donor. There are no real differences in energy for these π,π^* states upon switching between equatorial and axial conformers and the energies remain independent of solvent polarity. In marked contrast, the energy of the CT state depends on the molecular structure and the optimized geometry lies midway between axial and equatorial conformations. This optimized geometry is the most favorable structure for intramolecular charge transfer[8,9] and it is likely that the molecule adopts this shape before or during the charge-transfer step. Coupling between S_1 and CT states corresponds to an electronic coupling matrix element of 206 cm^{-1}. This is a relatively high value, partly because of the close proximity of donor and acceptor units, and is equivalent to k_BT at room temperature. Our calculations did not identify a clear role for the C−N stretching mode but $-CH_3$ rotation doubtless makes a contribution toward the nuclear reorganization energy.

Acknowledgment. We thank the EPSRC (GR/R23305) and the University of Newcastle for financial support.

References and Notes

(1) (a) Marcus, R. A. *J. Chem. Phys.* **1956**, *24*, 966. (b) Marcus, R. A.; Sutin, N. *Biochim. Biophys. Acta* **1985**, *811*, 265.

(2) Sumi, H.; Marcus, R. A. *J. Chem. Phys*. **1986**, *84*, 4894.

(3) (a) Dutton, P. L.; Alegria, G.; Gunner, M. R. *Biophys. J*. **1988**, *53A*, 206. (b) Johnson, A. E.; Tominga, K.; Walker, G. C.; Jarzeba, W.; Barbara, P. F. *Pure Appl. Chem*. **1993**, *65*, 1677. (c) Harriman, A.; Heitz, V.; Sauvage, J.-P. *J. Phys. Chem*. **1993**, *97*, 5940. (d) Gray, H. B.; Winkler, J. R. *J. Electroanal. Chem*. **1997**, *438*, 43. (e) Harriman, A. *Angew. Chem., Int. Ed.* **1999**, *38*, 945. (f) Chuev, G. N.; Lakhno, V. D.; Ustitnin, M. N. *J. Biol. Phys*. **2000**, *26*, 173. (g) Jeuken, L. J. C.; McEvoy, J. P.; Armstrong, F. A. *J. Phys. Chem. B* **2002**, *106*, 2304. (h) Fukuzumi, S.; Fujita, S.; Suenobu, T.; Yamada, H.; Imahori, H.; Araki, Y.; Ito, O. *J. Phys. Chem. A* **2002**, *106*, 1241.

(4) (a) Masad, A.; Huppert, D.; Kosower, E. M. *Chem. Phys*. **1990**, *144*, 391. (b) Leite, V. B. P. *J. Chem. Phys*. **1999**, *110*, 10067. (c) McHale, J. L. *Acc. Chem. Res*. **2001**, *34*, 265. (d) Zhang, Y. H.; Berg, M. A. *J. Chem. Phys*. **2001**, *115*, 4223. (e) Matyushov, D. V. *J. Chem. Phys.* **2001**, *115*, 8933. (f) Karmakar, R.; Samanta, A. *J. Phys. Chem. A* **2002**, *106*, 4447.

(5) (a) Ando, K. *J. Chem Phys.* **1994**, *101*, 2850. (b) Muegge, I.; Qi, P. X.; Wand, A. J.; Chu, Z. T.; Warshel, A. *J. Phys. Chem. B* **1997**, *101*, 825. (c) Yelle, R. B.; Ichiye, T. *J. Phys. Chem. B* **1997**, *101*, 4127. (d) Hayashi, S.; Kato, S. *J. Phys. Chem. A* **1998**, *102*, 3333. (e) Warshel, A. *J. Phys. Chem.* **1982**, *86*, 2218.

(6) (a) Bowler, B. E.; Raphael, A. L.; Gray, A. B. *Prog. Inorg. Chem. Bioinorg. Chem*. **1990**, *38*, 259. (b) Parson, W. W.; Chu, Z. T.; Warshel, A. *Biophys. J*. **1998**, *74*, 182. (c) Larsson, S. *Biochim. Biophys. Acta* **1998**, *1365*, 294. (d) Regan, J. J.; Onuchic, J. N. *Adv. Chem. Phys.* **1999**, *107*, 497.

(7) (a) Pourtois, G.; Beljonne, D.; Cornil, J.; Ratner, M. A.; Bredas, J. L. *J. Am. Chem. Soc*. **2002**, *124*, 4436. (b) Xue, Y. Q.; Datta, S.; Ratner, M. A. *J. Chem. Phys.* **2001**, *115*, 4292. (c) Wilkie, J.; Ratner, M. A.; Gerber, R. B. *J. Chem. Phys*. **1999**, *110*, 7610. (d) Bassler, H. *Polym. Adv. Technol.* **1998**, *9*, 402.

(8) (a) Lippert, E.; Luder, W.; Moll, F.; Nagele, W.; Boos, H.; Prigge, H.; Seibold-Blankenstein, I. *Angew. Chem*. **1961**, *73*, 695. (b) Lippert, E.; Rettig, W.; Bonacic-Koutecky, V.; Heisel, F.; Miehe, J. A. *Adv. Chem. Phys*. **1987**, *68*, 1. (c) Schuddeboom, W.; Jonker, S.; Warman, J.; Leinhos, U.; Kuhnle, W.; Zachariasse, K. *J. Phys. Chem.* **1992**, *96*, 10809. (d) Serrano-Andres, L.; Merchan, M.; Roos, B.; Lindh, R. *J. Am. Chem. Soc*. **1995**, *117*, 3189. (e) Rotkiewicz, K.; Grellmann, K. H.; Grabowski, Z. R. *Chem. Phys. Lett.* **1973**, *19*, 315. (f) Rettig, W. *Angew. Chem.* **1986**, *98*, 971.

(9) (a) Hashimoto, M.; Hamaguchi, H. *J. Phys. Chem*. **1995**, *99*, 7875. (b) Chudoba, C.; Kummrow, A.; Dreyer, J.; Stenger, J.; Nibbering, E. T. H.; Elsaesser, T.; Zachariasse, K. A. *Chem. Phys. Lett*. **1999**, *309*, 357. (c) Matousek, P.; Towrie, M.; Stanley, A.; Parker, A. W. *Appl. Spectrosc*. **1999**, *53*, 1485. (d) Kwok, W. M.; Ma, C.; Matousek, P.; Parker, A. W.; Phillips, D.; Towrie, M. *J. Phys. Chem. A* **2000**, *104*, 4188. (e) Okada, T.; Uesugi, M.; Kohler, G.; Rechthaler, K.; Rotkiewicz, K.; Rettig, W.; Grabner, G. *Chem. Phys*. **1999**, *241*, 327.

(10) Okamoto, H.; Kinoshita, M. *J. Phys. Chem. A* **2002**, *106*, 3485.

(11) (a) Grimme, S. *Chem. Phys. Lett*. **1996**, *259*, 128. (b) Parusel, A. B. J.; Köhler, G.; Grimme, S., *J. Phys. Chem. A* **1998**, *102*, 6297. (c) Evers, F.; Giraud-Giraud, J.; Grimme, S.; Manz, J.; Monte, C.; Oppel, M.; Rettig, W.; Saalfrank, P.; Zimmermann, P. *J. Phys. Chem. A* **2001**, *105*, 2911. (d) Parusel, A. B. J.; Schamschule, R.; Köhler, G. *Z. Phys. Chem*. **2002**, *216*, 361. (e) Parusel, A. B. J. *Chem. Phys. Lett*. **2001**, *340*, 531. (f) Letard, J. F.; Delmond, S.; Lapouyade, R.; Braun, D.; Rettig, W.; Kreissler, M. *Recl. Trav. Chim. Pay Bas* **1995**, *114*, 517.

(12) (a) Rauhut, G.; Clark, T.; Steinke, T. *J. Am. Chem. Soc*. **1993**, *115*, 9174. (b) Clark, T.; Bleisteiner, B.; Schneider, S. *J. Mol. Model*. **2002**, *8*, 87. (c) Engel, T.; Käb, G.; Lanig, H. *Z. Phys. Chem.* **2002**, *216*, 305.

(13) (a) Gedeck, P.; Scheider, S. *J. Photochem. Photobiol., A* **1999**, *121*, 7. (b) Gedeck, P.; Scheider, S. *J. Photochem. Photobiol., A* **1999**, *121*, 7. (c) Parusel, A. *J. Chem. Soc., Faraday Trans*. **1998**, *94*, 2923. (d) Broo, A. *Chem. Phys.* **1994**, *183*, 85.

(14) (a) Khalil, O. S.; Meeks, J. L.; McGlynn, S. P. *Chem. Phys. Lett*. **1976**, *39*, 458. (b) Rettig, W.; Bonacic-Koutecky, V. *Chem. Phys. Lett*. **1979**, *62*, 115. (c) Bangal, P. R.; Panja, S.; Chakravoti, S. *J. Photochem. Photobiol., A* **2001**, *139*, 5. (d) Bandyopadhyay, D.; Majumbar, D.; Das, K. K. *Theochem − J. Mol. Struct*. **1997**, *389*, 179.

(15) (a) Lipinski, J.; Chojnacki, H.; Grabowski, Z. R.; Rotkiewicz, K. *Chem. Phys. Lett*. **1980**, *70*, 449. (b) Majumdar, D.; Sen., R.; Bhattacharyya, K.; Bhattacharyya, S. P. *J. Phys. Chem*. **1991**, *95*, 4324. (c) Marguet, S.; Mialocq, J.-C.; Millie, P.; Berthier, G.; Momicchioli, F. *Chem. Phys*. **1992**, *160*, 265. (d) Belletete, M.; Nigam, S.; Durocher, G. *J. Phys. Chem*. **1995**, *99*, 4015. (e) Markovitsi, D.; Sigal, H.; Ecoftet, C.; Millie, P.; Charra, F.; Fiorini, C.; Nunzi, J. M.; Strzelecka, H.; Jallabert, C. *Chem. Phys*. **1994**, *182*, 69.

(16) (a) Grabowski, Z. R.; Rotkiewicz, K.; Siemiarczuk, A.; Cowley, D. J.; Baumann, W. *Nouv. J. Chim*. **1979**, *3*, 443. (b) Cowley, D. J.; Peoples, A. H. *J. Chem. Soc., Chem. Commun*. **1977**, 352. (c) LaFemina, J. P.; Duke, C. B.; Paton, A. *J. Chem. Phys*. **1987**, *87*, 2151.

(17) (a) Sobolewski, A. L.; Sudholt, W.; Domcke, W. *J. Phys. Chem. A* **1998**, *102*, 2716. (b) Sudholt, W.; Sobolewski, A. L.; Domcke, W. *Chem. Phys*. **1999**, *240*, 9. (c) Cornelissen-Gude, C.; Rettig, W. *J. Phys. Chem. A* **1999**, *103*, 4371. (d) Mennucci, B.; Toniolo, A.; Tomasi, J. *J. Am. Chem. Soc.* **2000**, *122*, 10621. (e) Zilberg, S.; Haas, Y. *J. Phys. Chem. A* **2002**, *106*, 1. (f) Parusel, A. B. J.; Rettig, W.; Sudholt, W. *J. Phys. Chem. A* **2002**, *106*, 804. (g) Manz, J.; Proppe, B.; Schmidt, B. *Phys. Chem. Chem. Phys*. **2002**, *4*, 1876. (h) Kafafi, S. A.; Lafemina, J. P.; Schenter, G. K. *Struct. Chem.* **1992**, *3*, 9.

(18) (a) Villani, A. *J. Chem. Phys*. **2002**, *117*, 1279. (b) Mancel, T.; Kleinekathofer, U.; May, V. *J. Chem. Phys*. **2002**, *117*, 636. (c) Tresadern, G.; McNamara, J. P.; Mohr, M.; Wang, H.; Burton, N. A.; Hillier, I. H. *Chem. Phys. Lett*. **2002**, *358*, 489. (d) Liao, J. L.; Voth, G. A. *J. Chem. Phys.* **2002**, *116*, 9174. (e) Tapia, O.; Fidder, H.; Safont, V. A.; Oliva, M.; Andres, J. *Int. J. Quantum Chem.* **2002**, *88*, 154.

(19) (a) Schenter, G. K.; Garrett, B. C.; Truhlar, D. G. *J. Phys. Chem. B* **2001**, *105*, 9672. (b) Warshel, A. *Acc. Chem. Res*. **2002**, *35*, 385. (c) Yamataka, H.; Aida, M.; Dupuis, M. *Chem. Phys. Lett.* **2002**, *353*, 310. (d) Skourtis, S. S.; Archontis, G.; Xie, Q. *J. Chem. Phys*. **2001**, *115*, 9444. (e) Harting, C.; Koper, M. T. M. *J. Chem. Phys*. **2001**, *115*, 8540. (f) Ungar, L. W.; Newton, M. D.; Voth, G. A. *J. Phys. Chem. B* **1999**, *103*, 7367.

(20) (a) Thoss, M.; Wang, H. B. *Chem. Phys. Lett*. **2002**, *358*, 298. (b) Balasubramanian, S.; Pal, S.; Bagchi, B. *Curr. Sci. India* **2002**, *82*, 845. (c) Egorov, S. A.; Denny, R. A.; Reichman, D. R. *J. Chem. Phys.* **2002**, *116*, 5080.

(21) (a) In the archetypal case of intramolecular charge transfer, namely, 4-dimethylaminobenzonitrile, the light-induced, charge-transfer process has been variously described as involving a twisted intramolecular charge-transfer (TICT) state (ref 8f), a wagged ICT (ref 8d), a planar ICT (ref 21b), and a rehydribization ICT (ref 21c). (b) Zachariasse, K. A.; Grobys, M.; Van der Haar, T.; Hebecker, A.; Ilchev, Y. V.; Jiang, Y.-B.; Morewski, O.; Kuhnle, W. *J. Photochem. Photobiol., A* **1996**, *102*, 59. (c) Sobolewski, A. L.; Sudholt, W.; Domcke, W. *Chem. Phys. Lett*. **1996**, *259*, 119.

(22) Brun, A. M.; Harriman, A.; Tsuboi, Y.; Okada, T.; Mataga, N. *J. Chem. Soc., Faraday Trans.* **1995**, *91*, 4047.

(23) (a) Mordasini Denti, T. Z.; Beutler, T. C.; van Gunsteren, W. F.; Diederich, F.; *J. Phys. Chem*. **1996**, *100*, 4256. (b) Okuno Y. *J. Am. Chem. Soc.* **2000**, *122*, 2925.

(24) (a) Jakobsen, S.; Mikkelsen, K. V.; Pedersen, S. U. *J. Phys. Chem.* **1996**, *100*, 7411. (b) Bader, J. S.; Cortis, C. M.; Berne, B. J. *J. Chem. Phys.* **1997**, *106*, 2372. (c) Clark, C. D.; Hoffman, M. Z. *J. Phys. Chem. A.* **1997**, *101*, 1782. (d) Vath, P.; Zimmt, M. B.; Matyushov, D. V.; Voth, G. A. *J. Phys. Chem. B* **1999**, *103*, 9130. (e) Rosso, K. M.; Rustad, J. R. *J. Phys. Chem. A* **2000**, *104*, 6718.

(25) Wasielewski, M. R.; Minsek, D. W.; Niemczyk, M. P.; Svec, W. A.; Yang, N. C. *J. Am. Chem. Soc.* **1990**, *112*, 2823.

(26) Rettig, W.; Haug, R.; Wirz, J. *Chem. Phys. Lett*. **1991**, *180*, 216.

(27) (a) Stewart J. J. P. *J. Comput. Chem.* **1989**, *10*, 209. (b) Stewart J. J. P. *J. Comput. Chem.* **1989**, *10*, 221.

(28) Fujitsu Limited, 1989−2000 Oxford Molecular Ltd.

(29) Frisch, M. J.; Trucks, G. W.; Schlegel, H. B.; Scuseria, G. E.; Robb, M. A.; Cheeseman, J. R.; Zakrzewski, V. G.; Montgomery, J. A., Jr.; Stratmann, R. E.; Burant, J. C.; Dapprich, S.; Millam, J. M.; Daniels, A. D.; Kudin, K. N.; Strain, M. C.; Farkas, O.; Tomasi, J.; Barone, V.; Cossi, M.; Cammi, R.; Mennucci, B.; Pomelli, C.; Adamo, C.; Clifford, S.;

Ochterski, J.; Petersson, G. A.; Ayala, P. Y.; Cui, Q.; Morokuma, K.; Malick, D. K.; Rabuck, A. D.; Raghavachari, K.; Foresman, J. B.; Cioslowski, J.; Ortiz, J. V.; Baboul, A. G.; Stefanov, B. B.; Liu, G.; Liashenko, A.; Piskorz, P.; Komaromi, I.; Gomperts, R.; Martin, R. L.; Fox, D. J.; Keith, T.; Al-Laham, M. A.; Peng, C. Y.; Nanayakkara, A.; Challacombe, M.; Gill, P. M. W.; Johnson, B.; Chen, W.; Wong, M. W.; Andres, J. L.; Gonzalez, C.; Head-Gordon, M.; Replogle, E. S.; Pople, J. A. *Gaussian 98*, revision A.9; Gaussian Inc.: Pittsburgh, PA, 1998.

(30) (a) Binkley, J. S.; Pople, J. A.; Hehre, W. J. *J. Am. Chem. Soc.* **1980**, *102*, 939. (b) Gordon, M. S.; Binkley, J. S.; Pople, J. A.; Pietro, W. J.; Hehre, W. J. *J. Am. Chem. Soc.* **1982**, *104*, 2797. (c) Pietro, W. J.; Franck, M. M.; Hehre, W. J.; Defrees, D. J.; Pople, J. A.; Binkley, J. S. *J. Am. Chem. Soc*. **1982**, *104*, 5039. (d) Dobbs, K. D.; Hehre, W. J. *J. Comput. Chem.* **1986**, *7*, 359. (e) Dobbs, K. D.; Hehre, W. J. *J. Comput. Chem.* **1987**, *8*, 861. (f) Dobbs, K. D.; Hehre, W. J. *J. Comput. Chem.* **1987**, *8*, 880.

(31) (a) Sharp, K.; Honig, B. *Annu. Rev. Biophys. Biophys. Chem.* **1990**, *19*, 301. (b) Sitkoff, D.; Sharp. K. A.; Honig, B. *J. Phys. Chem.* **1994**, *98*, 1978.

(32) Accelrys Inc.

(33) Brooks, B. R.; Bruccoleri, R. E.; Olafson, B. D.; States D. J.; Swaminathan, S.; Karplus, M. *J. Comput. Chem.* **1983**, *4*, 187.

(34) Herbach, J.; Waluk, J. *Chem. Phys*. **1993**, *176*, 467.

(35) Berlman, I. B., *J. Chem. Phys*. **1970**, *52*, 5616.

(36) Birks, J. B. In *Photophysics of Aromatic Molecules*; Wiley: New York, 1970.

(37) (a) Dewar, M. J. S.; Thiel W. *J. Am. Chem. Soc*. **1977**, *99*, 4499. (b) Davis, L. P. *J. Comput. Chem.* **1981**, *2*, 433. (c) Dewar, M. J. S.; McKee, M. L.; Rzepa, H. S. *J. Am. Chem. Soc*. **1978**, *100*, 3607. (d) Dewar, M. J. S.; Zoebisch, E. G.; Healy, E. F. *J. Am. Chem. Soc.* **1985**, *107*, 3902. (e) Dewar, M. J. S.; Reynolds, C. H. *J. Comput. Chem.* **1986**, *2*, 140.

(38) Foresman, J. B.; Head-Gordon, M.; Pople, J. A.; Frisch, M. J. *J. Phys. Chem*. **1992**, *96*, 135.

(39) Nina, M.; Beglov, D.; Roux, B. *J. Phys. Chem.* **1997**, *106*, 5239.

(40) (a) Warshel, A. *J. Phys. Chem.* **1982**, *86*, 2218. (b) Tachiya, M. *J. Phys. Chem.* **1989**, *93*, 7050. (c) King, G.; Warshel, A. *J. Chem. Phys*. **1990**, *93*, 8682. (d) Nonella, M.; Schulten, K. *J. Phys. Chem*. **1991**, *95*, 2059. (e) Schulten, K.; Tesch, M. *Chem. Phys*. **1991**, *158*, 421. (f) Treutlein, H.; Schulten, K.; Brunger, A. T.; Karplus, M.; Deisenhofer, J.; Michel, H. *Proc. Natl. Acad. Sci. U.S.A.* **1992**, *89*, 75.

(41) Jorgensen, W. L.; Chandrasekhar, J.; Madura, J.; Impev, R. W.; Klein, M. L. *J. Chem. Phys.* **1983**, *79*, 926.

(42) Ortega, J.; Rheinboldt, W. In *Iterative Solution of Nonlinear Equations in Several Variables*; Academic Press: New York, 1970.

(43) Chita, R.; Smith, P. E. *J. Phys. Chem. B* **2000**, *104*, 5854.

(44) McConnell, H. M. *J. Chem. Phys.* **1961**, *35*, 508.

(45) (a) Onuchic, J. N.; de Andrade, C. P.; Beratan, D. N. *J. Chem. Phys*. **1991**, *95*, 1131. (b) Balabin, I. A.; Onuchic, J. N. *J. Phys. Chem.* **1996**, *100*, 11573.

(46) (a) Gruschus, J. M.; Kuki, A. *J. Phys. Chem.* **1993**, *97*, 5581. (b) Siddarth, P.; Marcus, R. A. *J. Phys. Chem.* **1993**, *97*, 2400. (c) Regan, J. J.; Risser, S. M.; Beratan, D. N.; Onuchic, J. N. *J. Phys. Chem*. **1993**, *97*, 13083. (d) Stuchebrukhov, A. A.; Marcus, R. A. *J. Chem. Phys.* **1995**, *99*, 7581. (e) Gehlen, J. N.; Daizadeh, I.; Stuchebrukhov, A. A.; Marcus, R. A. *Inorg. Chim. Acta* **1996**, *243*, 271. (f) Medvedev, D. M.; Daizadeh, I.; Stuchebrukhov, A. A. *J. Am. Chem. Soc.* **2000**, *122*, 6571.

(47) (a) Wolfgang, J.; Risser, S. M.; Priyadarshy, S.; Beratan, D. N. *J. Phys. Chem. B* **1997**, *101*, 2986. (b) Daizadeh, I.; Medvedev, E. S.; Stuchebrukhov, A. A. *Proc. Natl. Acad. Sci. U.S.A.* **1997**, *94*, 3703. (c) Balabin, I. A.; Onuchic, J. N. *Science* **2000**, *290*, 114.

(48) Economou, E. N. In *Green's Functions in Quantum Physics*, 2nd ed.; Springer: New York, 1983.

(49) (a) Jones, G. A.; Carpenter, B. K.; Paddon-Row, M. N. *J. Am. Chem. Soc*. **1999**, *121*, 11171. (b) Jones, G. A.; Carpenter, B. K.; Paddon-Row, M. N. *J. Am. Chem. Soc*. **1998**, *120*, 5499.

(50) Gomez, M. A.; Pratt, L. R. *J. Chem. Phys*. **1998**, *109*, 8783.

(51) Masad, A.; Huppert, D.; Kosower, E. M. *Chem. Phys.* **1990**, *144*, 391.